AIP | Journal of Applied Physics

Shape transition of unstrained flattest single-walled carbon nanotubes under pressure

Weihua Mu, Jianshu Cao, and Zhong-can Ou-Yang

Citation: Journal of Applied Physics **115**, 044512 (2014); doi: 10.1063/1.4863455
View online: http://dx.doi.org/10.1063/1.4863455
View Table of Contents: http://scitation.aip.org/content/aip/journal/jap/115/4?ver=pdfcov
Published by the AIP Publishing

Shape transition of unstrained flattest single-walled carbon nanotubes under pressure

Weihua Mu,[1,2,3,a)] Jianshu Cao,[1,4,b)] and Zhong-can Ou-Yang[2,3,4,5]
[1]*Department of Chemistry, Massachusetts Institute of Technology, Cambridge, Massachusetts 02139, USA*
[2]*State Key Laboratory of Theoretical Physics, Institute of Theoretical Physics, The Chinese Academy of Sciences, P. O. Box 2735 Beijing 100190, China*
[3]*Kavli Institute for Theoretical Physics China, The Chinese Academy of Sciences, P. O. Box 2735 Beijing 100190, China*
[4]*Singapore-MIT Alliance for Research and Technology (SMART), Singapore 138602*
[5]*Center for Advanced Study, Tsinghua University, Beijing 100084, China*

(Received 2 December 2013; accepted 15 January 2014; published online 30 January 2014)

Single walled carbon nanotube's (SWCNT's) cross section can be flattened under hydrostatic pressure. One example is the cross section of a single walled carbon nanotube successively deforms from the original round shape to oval shape, then to peanut-like shape. At the transition point of reversible deformation between convex shape and concave shape, the side wall of nanotube is flattest. This flattest tube has many attractive properties. In the present work, an approximate approach is developed to determine the equilibrium shape of this unstrained flattest tube and the curvature distribution of this tube. Our results are in good agreement with recent numerical results, and can be applied to the study of pressure controlled electric properties of single walled carbon nanotubes. The present method can also be used to study other deformed inorganic and organic tube-like structures. © *2014 AIP Publishing LLC*. [http://dx.doi.org/10.1063/1.4863455]

I. INTRODUCTION

Carbon nanotubes (CNTs) have superior mechanical properties due to strong carbon-carbon atomic interactions in their honeycomb lattices.[1] CNTs' high elastic modulus, exceptional axial stiffness, and low density, make them ideal for nanotechnology applications.[2] CNTs' mechanical properties are highly anisotropic, and have been studied extensively.[3,4] In contrast to the high tensile strength,[5] CNTs are susceptible to mechanical distortion in their radial directions under applied hydrostatic pressure on the order of GPa.[6–17] The radial deformation controlled by the applied pressure provides an approach to modify the electronic properties of single walled carbon nanotube (SWCNTs),[18] consequently, radial deformation of SWCNTs can be observed by optical spectroscopy since the electronic band structure of a SWCNT is sensitive to its morphological transition.[4,19] In addition, a SWCNT's chemical reactivity depends on its mechanical deformations,[20–22] which plays the key role in the design of CNT-based gas sensors.[23]

Among the radially deformed SWCNTs, the fully collapsed structure with two strained edges bridged by a flat middle section[24–27] attracts intense interest because of its physical and chemical properties[28–30] associated with its flat ribbon-like middle part.[30] However, the fully collapsed SWCNTs are stabilized by van der Walls (vdW) interaction between two opposing flat walls (with typical interlayer distance $d_0 \approx 3.4$ Å) leads to irreversible collapsing. The vdW interaction may also induce twist and bending of the flat section in a fully collapsed SWCNT. Moreover, the edge section of a collapsed SWCNT is highly strained. As it is widely known, with the increase of hydrostatic pressure, a cylindrical SWCNT at first becomes oval-shaped, and then becomes peanut-shaped.[15] Between these two shapes, there exists a critical shape under certain pressure which is the unstrained flattest configuration of SWCNTs. The radially deformed SWCNT with a flat section that is similar to fully collapsed SWCNTs have advantages over fully collapsed ones: (1) it can be shifted back to the state with a circular cross section reversibly; (2) there is no twist in the flat section since vdW interaction can be neglected; (3) there is no strain in the two edges, therefore avoiding the strain-induced change of the electronic band structure.

II. MODEL

In the present manuscript, we will theoretically determine the shapes of the unstrained flattest SWCNTs. Although the problem has been studied by molecular dynamical simulations and numerical calculations,[15] there still lacks the analytical explicit expressions which can provide a design principle for CNT-based devices. We will accomplish this task by carefully studying the transition of the SWCNT deforming from a convex shape to a concave shape, and giving an analytical expression of the critical shape for an unstrained flattest tube. Based on this analytical expression, we can calculate the critical pressure for the unstrained flattest SWCNTs. We will also discuss the curvature effect for the orbital hybridization of carbon atoms on the sidewall of the SWCNT. The latter is important for studying the absorption of molecules on SWCNTs. Although the deformation of the SWCNT investigated in the present work is in ideal conditions, the results can be used as the theoretical limits for the actual CNT-devices.

The equilibrium shape of deformed SWCNTs is determined by minimizing the free energy under certain constraints. In the present problem, the free energy contains the elastic

[a)]Electronic addresses: whmu@mit.edu and muwh@itp.ac.cn
[b)]Electronic mail: jianshu@mit.edu

energy and the pressure term, $F_b = E_b + p\,\Delta V$. Although both bond bending and bond stretching contribute to the elastic energy of SWCNTs, at the energy scale $\Delta p \cdot V_0 \sim 1\,\text{eV} \approx k_c$ (k_c is the bending stiffness of SWCNTs[31,32]), the bond bending effect predominates.[33] The bond-bending energy of a SWCNT can be described by its curvatures[24,33]

$$E_b = \frac{k_c}{2}\oint (2H)^2\, dA + \bar{k}\oint K\, dA. \tag{1}$$

Here, H and K are the mean curvature and Gaussian curvature of the surfaces of carbon atoms, and $k_c = 1.17\,\text{eV}$ (Ref. 33) is consistent with the result of Tersoff *et al.*[31] The expression of free energy can be mapped to 2D. Consider a straight SWCNT with radius $\rho(\phi)$, without the inclusion of its two end-caps, the surface of the tube can be described in cylindrical coordinates as, $\vec{r}(\phi, l) = \{\rho(\phi)\cos\phi,\ \rho(\phi)\sin\phi,\ l\}$. Here, $0 \le \phi < 2\pi$, and $0 \le L \le L_0$, with L_0 the length of straight tube axis. The origin of ρ is arbitrary. The surface's mean and Gaussian curvature are $2H = -\left(\rho^2 + 2\rho'^2 - \rho\rho''\right)\left(\rho^2 + \rho'^2\right)^{3/2}, K = 0$. Comparing with the relative curvature $k_r = \left|\left(\rho^2 + 2\rho'^2 - \rho\rho''\right)\right|/\left(\rho^2 + \rho'^2\right)^{3/2}$ of a plane curve $\rho = \rho(\phi)$, the bending energy can be rewritten as $E_b = k_c L_0/2\oint k_r^2 ds$, where s the arc parameter of boundary curve $\mathcal{C}: \rho(\phi)$, and line element $\mathrm{d}s = [\rho^2 + (\mathrm{d}\rho/\mathrm{d}\phi)^2]^{1/2}\mathrm{d}\phi$.

The equilibrium shape of a deformed SWCNT is the solution of the 2D variation problem $\delta^{(1)}F = 0,\ \delta^{(2)}F > 0$, with

$$F = \frac{k_c}{2}\oint k_r^2(s)\mathrm{d}s + p\int \mathrm{d}A + \lambda\left[l_0 - \oint \mathrm{d}s\right], \tag{2}$$

where λ is the Lagrange multiplier, which is introduced to keep the tube circumference at constant l_0. Distorting the curve $\mathcal{C}$ by a small perturbation $\psi(s)$ along the normal direction of the curve, the variations in $\delta^{(1)}F$ are

$$\begin{aligned}
\delta^{(1)}\oint \mathrm{d}s &= -\oint \mathrm{d}s\, k_r(s)\psi(s),\\
\delta^{(1)}\oint \mathrm{d}s\, k_r^2(s) &= \oint \mathrm{d}s\,\left[k_r^3(s) + 2k_r''(s)\right]\psi(s),\\
\delta^{(1)}\oint \mathrm{d}A &= \oint \mathrm{d}s\,\psi(s),
\end{aligned} \tag{3}$$

which can be obtained in a simple way, as shown in Appendix A. Then, the equation for the equilibrium shape of SWCNTs is obtained

$$p + \frac{k_c}{2}\,k_r(s)^3 + k_c k_r''(s) + \lambda k_r(s) = 0. \tag{4}$$

Obviously, there is a special solution corresponding to the tube of circular cross-section, $k_r = 1/\rho_0$, which implies the necessary condition for maintaining SWCNT's circular cross section. The initial equation of Eq. (4)

$$p\,k_r + \frac{k_c}{8}\,k_r^4 + \frac{k_c}{2}(k_r')^2 + \frac{\lambda}{2}k_r^2 = c_1, \tag{5}$$

leads to the equation of k_r

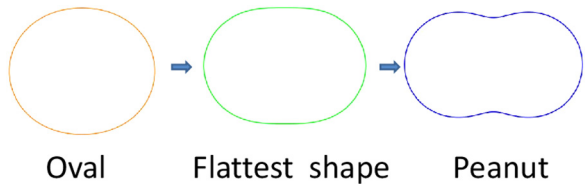

FIG. 1. Illustration of shape transitions for a cross section of SWCNT with C_{2v} symmetry. The critical shape for the transition from the oval shape to the peanut-like shape is the unstrained flattest shape of SWCNT.

$$k_r' = \pm\sqrt{c_2 + \alpha k_r - \beta k_r^4 + \gamma k_r^2}, \tag{6}$$

with $\alpha \equiv -2p/k_c,\ \beta = 1/4, \gamma \equiv -\lambda/k_c$.

Under hydrostatic pressure, the tube of circular cross-section tube can be deformed to a convex structure with lower symmetry C_{nv}. With the increase of pressure, the curvature changes continually from $k_r > 0$ (convex shape) to $k_r < 0$ (concave shape). A critical shape for the transition from convex to concave satisfies $k_r \ge 0$, with the minimal curvature being exactly zero, $k_{r,\min} = 0$. The critical shape is the flattest shape for unstrained SWCNTs. In particular, for the deformed SWCNT with C_{2v} symmetry, the convex shape is the "oval" shape, and concave shape is "peanut-like" shape, as shown in Fig. 1. Equation (6) can be solved numerically by iteration.[15] Due to the symmetry of the deformed shape, only a quarter of the curve $\mathcal{C}$ need to be considered, as shown in Fig. 2. For convenience, the length of curve $\mathcal{C}$ is re-scaled to 2π. The $k_r(s = \pi/2) = 0$ and the inextensible condition $l_0 = 2\pi$ lead to a constraint

$$\frac{\pi}{2} = \int_{k_{r,max}}^{0} \frac{\mathrm{d}k_r}{\sqrt{c_2 + \alpha k_r - \beta k_r^4 + \gamma k_r^2}}. \tag{7}$$

The direction of tangential line changes from $\theta = \pi/2$ to $\theta = 0$, as the arc parameter s changes from 0 to $\pi/2$, which provides another independent equation

$$-\frac{\pi}{2} = \int_{k_{r,max}}^{0} \frac{k_r \mathrm{d}k_r}{\sqrt{c_2 + \alpha k_r - \beta k_r^4 + \gamma k_r^2}}. \tag{8}$$

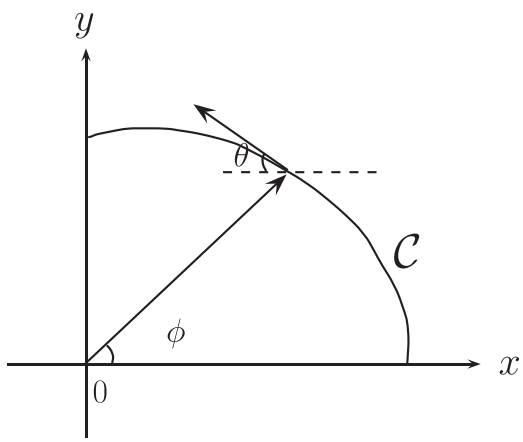

FIG. 2. Illustration of a quarter of the deformed cross section of a SWCNT with C_{2v} symmetry. The θ is the angle between x-axis and the direction of the curve $\mathcal{C}$'s tangential line. The ϕ is the polar angle.

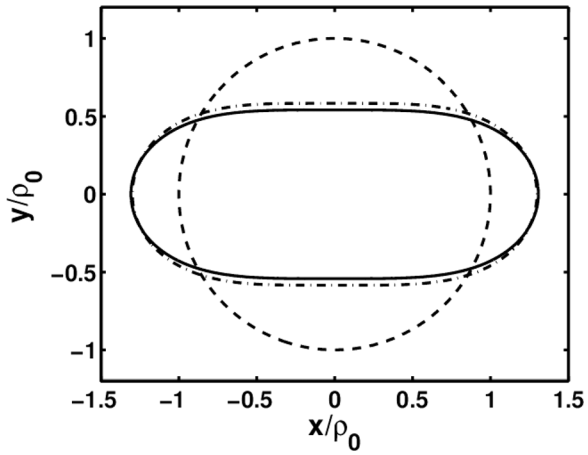

FIG. 3. Comparison of the explicit solution and exact solution of deformed SWCNTs' at the critical flattest shape with C_{2v} symmetry. The solid line curve is the present explicit approximate solution of the shape equation, the dashed-dotted line curve is the exact numerical solution, and the dashed line is unperturbed circular shape of a SWCNT. The ρ_0 is the radius of the SWCNT without the deformation.

Equations (7) and (8) can be calculated self-consistently. The relation $d\theta = k_r ds$ is used in the derivation of Eq. (8). In principle, the flattest shape with high order symmetries (C_{nv}, $n \geq 3$) can be obtained similarly.

In the application of deformed SWCNT related devices, such as a gas sensor, it is necessary to derive an explicit expression of the critical pressure for the flattest shape as the design guideline for working conditions. In this study, we will give an analytical solution for that.

III. CALCULATION

Based on the numerical result of k_r, we know that c_0 is very small. Thus $\gamma = 0$ is a good initial guess for the self-consistent of shape equations. (7) and (8). We get an approximate solution with $\gamma = 0$, and then compare it with the numerical solution to check the consistency. For $\gamma = 0$, $k_{r,\min} = 0$, Eq. (6) implies $c_2 = 0$, it can be reduced to

$$\frac{dk_r}{\sqrt{\alpha k_r - \beta k_r^4}} = ds = \frac{1}{k_r} d\theta, \tag{9}$$

with the additional necessary condition of equilibrium critical shape: k_r reaches its maximum at $\theta = \pi/2$, and its minimum at $\theta = \pi/2 + \pi/n$. Thus, we have, $k_{r,n}(\theta) = (4\alpha)^{(1/3)} \sin^{2/3}[3(\theta + c_1(n))/4]$ and $c_1(n)(\theta) = 5\pi/6 - \pi/n$, (see Appendix B for the details). The constant length of curve $\mathcal{C}$, $l_0 = 2\pi$ requires

$$\frac{l_0}{2n} = \frac{\pi\rho_0}{n} = (4\alpha)^{(-1/3)} \int_{\pi/2}^{\pi/2+\pi/n} k_{r,n}^{-1}(\theta)\, d\theta = \frac{c_2(n)}{(4\alpha)^{(1/3)}}. \tag{10}$$

The constants $c_2(n)$ can be derived as

$$c_2(n) = \frac{4\sqrt{\pi}\Gamma\left(\frac{7}{6}\right)}{\Gamma\left(\frac{2}{3}\right)} - \frac{4}{3}\left[{}_2F_1\left(\frac{1}{2}, \frac{5}{6}, \frac{3}{2}, \cos^2\frac{3\pi}{4n}\right)\cos\left(\frac{3\pi}{4n}\right)\right].$$

Here, ${}_2F_1(a, b, c, z)$ is the hypergeometric function.[34] Some constants $c_2(n)$ for a unstrained flattest tube with C_{nv} symmetries are listed in Table I. The curvature $k_r(n), n \geq 2$ has the form of

$$k_{r,n}(\theta) = \left(\frac{n\, c_2(n)}{\pi\rho_0}\right) \sin^{2/3}\left[\frac{3}{4}\left(\theta + \frac{5\pi}{6} - \frac{\pi}{n}\right)\right]. \tag{11}$$

In particular, $c_2(2) = 4.3244$, predicts the critical shape for the transition from oval-shaped tube to peanut-like shape.

The equilibrium shape of the unstrained flattest SWCNTs with C_{2v} symmetry can be described by parametric equations (see Appendix C for the details)

$$\begin{cases} x_2(\theta) = \dfrac{2\pi\rho_0}{c_2} \sin\left(\dfrac{\theta}{4} + \dfrac{\pi}{4}\right) \sin^{1/3}\left(\dfrac{3\theta}{4} + \dfrac{\pi}{4}\right), \\ y_2(\theta) = \dfrac{2\pi\rho_0}{c_2} \left[\dfrac{\sin^{2/3}\left(\dfrac{\pi}{8}\right)}{\sqrt{2}} + \sin\left(\dfrac{\theta}{4} - \dfrac{\pi}{4}\right) \sin^{1/3}\left(\dfrac{3\theta}{4} + \dfrac{\pi}{4}\right)\right]. \end{cases} \tag{12}$$

The comparison of the explicit result and the exact result is shown in Fig. 3.

The cross-sectional area of the tube is

$$S_2 = \frac{1}{2}\left(\frac{\pi\rho_0}{c_2}\right)^2 \int_{\pi/2}^{\pi} \frac{\sin\theta \sin(\theta/4 + \pi/4)}{\sin^{1/3}(3\theta/4 + \pi/4)} = 2.449\rho_0^2. \tag{13}$$

Comparing with the undistorted tube, $S_0 = \pi\rho_0^2$, the geometric constant is $\mathcal{G} = S_2/S_0 = 0.78$, which is in good accordance with the exact value $\mathcal{G} = 0.8195$.[15]

The curvature distribution characterizes the flatness of the deformed SWCNTs. The curvature distribution provides useful information about the bond hybridization of SWCNTs, which governs the gas-absorbing ability of SWCNTs. We compare the curvature distributions of our approximate result and the exact solution, as shown in Fig. 4. The exact curvature distribution can be calculated self-consistently according to Eqs. (7) and (8). The hybrid orbital of carbon atoms in the SWCNT is sensitive to the local curvature of the tube. For a SWCNT, in the local coordinate of a given carbon atom i, the three neighbours of the center atom i have coordinates[32]

$$\begin{aligned} x_{0j} &= \cos\theta_j - \frac{(a_0/R)^2}{3} \sin^4\theta_j \cos\theta_j, \\ y_{0j} &= \sin\theta_j + \frac{(a_0/R)^2}{6} \sin^3\theta_j \cos(2\theta_j), \quad j = 1, 2, 3, \\ z_{0j} &= \frac{(a_0/R)}{2} \sin^2\theta_j, \end{aligned} \tag{14}$$

with $\theta_1 = \theta_c$, $\theta_2 \approx \theta_c + 2\pi/3$, and $\theta_2 = \theta_c + 4\pi/3$ being the angles between bond curves and the direction of the tube axis, at the position of atom i.[33] Here, $a_0 = 1.42$ Å is the equilibrium bond length of carbon-carbon bond, R is the

TABLE I. The c_2 values for the approximate solution of a unstrained flattest SWCNT whose cross section has C_{nv} symmetry.

n	2	3	4	5	6	7	8	9	10
c_2	4.324	3.728	3.372	3.124	2.936	2.788	2.665	2.562	2.473

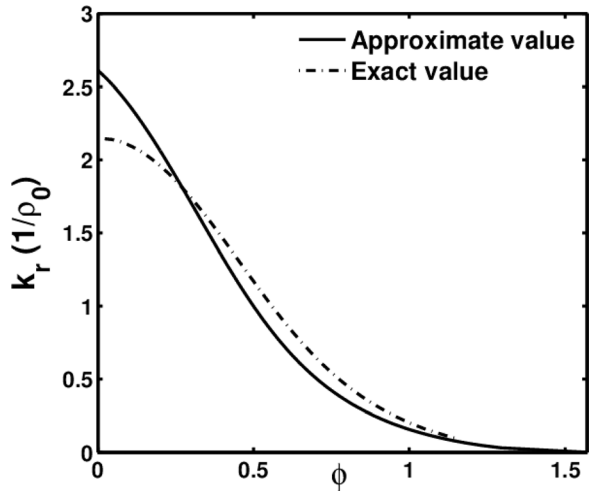

FIG. 4. Comparing the approximate and exact results of the curvature distribution of unstrained SWCNTs at the transition from oval to peanut shape. Here, ϕ is the polar angle as shown in Fig.2. The curvature k_r is in the unit of $1/\rho_0$, with ρ_0 being the radius of unperturbed circular cross section of a SWCNT.

radius of the SWCNT, a_0/R characterizes the curvature dependent properties of SWCNTs. The distance between atom i and their three neighbours can be described as $r_{ij}^0 = 1 - \frac{(a_0/R)^2}{24}\sin^4\theta_j$. The directions (the direction of symmetry axis) for the three sp^2 orbits can be written as $\hat{e}_j = \{x_{0j}, x_{0j}, z_{0j}\}/r_{ij}^0$.

In the local coordinate system associated with the give carbon atom i, the π orbit and three sp^2 orbits can be decomposed as, $|\pi\rangle = c_1|2s\rangle + \sqrt{1-c_1^2}\,|2p_z\rangle$, and $|sp^2\rangle_j = c_2\,|2s\rangle + \sqrt{1-c_2^2}\,(e_{jk}|2p_k\rangle)$, $k=x,y,z$. with, $c_1 = \sqrt{\frac{6\alpha_0^2}{32-3\alpha_0}} \approx \frac{\sqrt{3}}{4}\alpha_0$, $c_2 = \sqrt{\frac{32-9\alpha_0^2}{3(32-3\alpha_0^2)}} \approx \frac{1}{\sqrt{3}}\left(1-\frac{3}{32}\alpha_0^2\right)$, and $\alpha_0 \equiv a_0/R$. Therefore, $|\pi(\alpha_0)\rangle = \frac{\sqrt{3}}{4}\alpha_0|2s\rangle + \left(1-\frac{3}{32}\alpha_0^2\right)|2p_z\rangle$, which plays a key role in the electronic and chemical properties of SWCNTs.[20] For graphene, $|\pi(\alpha_0=0)\rangle = |2p_z\rangle$. By adjusting applied hydrostatic pressure, the $|\pi\rangle$ at the main part of a SWCNT can be switched between $|\pi(\alpha_0)\rangle$ and $|2p_z\rangle$ reversibly.

IV. CONCLUSION

In summary, we have theoretically investigated the unstrained flattest shape of SWCNT under hydrostatic pressure, which can recover to its original circular cross-section after withdrawing the pressure. We find a good approximate solution for the shape of this flattest SWCNT, and theoretically determine the curvature distribution. We also discuss the curvature-dependent hybrid orbital of the SWCNT. The present analytical solution is in good agreement with the exact numerical solution, and it can be used as the design guideline in CNT-based nano-electronic devices. Our approach can be generalized to investigate other inorganic and organic elastic membrane systems,[35–37] including the self-assembled polymer materials and colloidal aggregations.[38,39] In the actual devices, the deformed SWCNT may be supported by the substrate. The present results provide the theoretical boundary for this CNT-based devices. It is worth noting that the variations in Eq. (3) can also been obtained in other approaches.[40,41]

ACKNOWLEDGMENTS

W. Mu and J. Cao acknowledge the financial assistance of Singapore-MIT Alliance for Research and Technology (SMART), National Science Foundation (NSF CHE-112825). W. Mu and Z-c. Ou-Yang acknowledge the support of National Science Foundation of China (NSFC) (Grants Nos. 11074259 and 11374310), and the Major Research Plan of the National Natural Science Foundation of China (Grant No. 91027045). J. Cao has been partly supported by the Center for Excitonics, an Energy Frontier Research Center funded by the U.S. Department of Energy, Office of Science, Office of Basic Energy Sciences under Award No. DE-SC0001088. W. Mu thanks Dr. Linying Cui for modifying the manuscript.

APPENDIX A: THE DETAILS OF VARIATIONAL CALCULATIONS

We will show the details of deriving the variations in Eqs. (3). The curve is shown in Fig. 5.

1. $\delta^{(1)}\oint ds$

With the distorsion $\psi(s)$ along the normal direction of the closed boundary curve, the plane boundary curve $\mathcal{C}$ becomes

$$\vec{r}(s) \to \vec{r}(s) + \psi(s)\hat{n}(s),$$

with $\hat{n}$ the normal direction of the curve $\mathcal{C}: \vec{r}(s)$, and s the arc parameter. The line element

$$\begin{aligned} ds = |\vec{r}'(s)|ds &\to \left|\frac{d\vec{r}(s)}{ds} + \frac{d(\psi(s)\hat{n}(s))}{ds}\right| ds, \\ &= |(1-k_r(s)\psi(s))\hat{t}(s) + \psi'(s)\hat{n}(s)|ds, \\ &= \sqrt{(1-k_r(s)\psi(s))^2 + \psi'^2(s)}\,ds, \\ &= (1-k_r(s)\psi(s))ds + O\left(\psi^2(s)\right). \end{aligned} \tag{A1}$$

The length of the $\mathcal{C}$ becomes

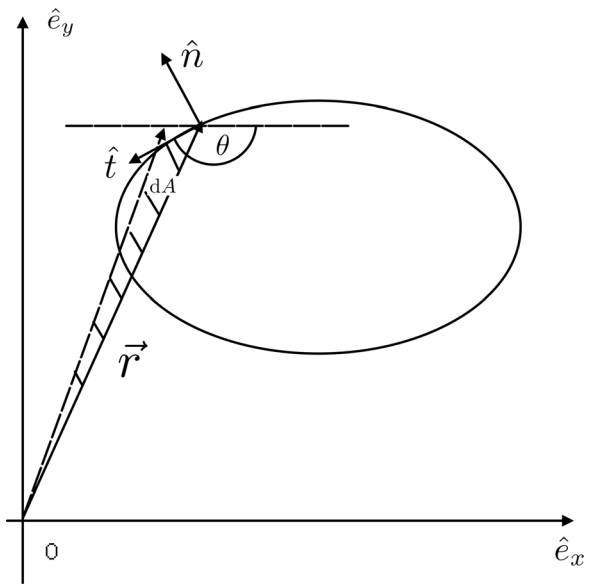

FIG. 5. A general closed curve.

$$\oint \mathrm{d}s = \oint (1 - k_r(s)\psi(s))\mathrm{d}s + O\left(\psi^2(s)\right). \tag{A2}$$

Here, we have used the relation between the tangent and normal vector of a plane curve

$$\hat{t}(s) \equiv \frac{\mathrm{d}\vec{r}(s)}{\mathrm{d}s},\ \hat{t}\,'(s) = k_r(s)\hat{n}(s),\ \hat{n}'(s) = -k_r(s)\hat{t}(s),$$

and $'$ denoted $\mathrm{d}/\mathrm{d}s$. Thus, the first order variation of the length of curve $\mathcal{C}$ has the form

$$\delta^{(1)}\oint \mathrm{d}s = -\oint k_r(s)\psi(s)\mathrm{d}s.$$

2. $\delta^{(1)}\oint k_r^2 \mathrm{d}s$

With the distorsion $\vec{r}(s) \to \vec{r}(s) + \psi(s)\hat{n}(s)$, the s is not the arc parameter of the deformed curve $\vec{r}'(s)$, the curvature changes to

$$\begin{aligned} k_r(s) \to \frac{|\vec{r}'(s) \times \vec{r}''(s)|}{|\vec{r}'(s)|^3} &= \frac{k_r + \psi''(s) - 2k_r^2(s)\psi(s)}{(1 - k_r(s)\psi(s))^3} + O\left(\psi^2(s)\right), \\ &= k_r(s) + k_r^2(s)\psi(s) + \psi''(s) + O\left(\psi^2(s)\right). \end{aligned} \tag{A3}$$

Here, we have used the relations

$$\begin{aligned} \vec{r}'(s) &\to (1 - k_r(s)\psi(s))\mathrm{d}s + O\left(\psi^2(s)\right), \\ \vec{r}''(s) &\to (-k_r'(s) - 2k_r(s)\psi'(s))\hat{t}(s) \\ &\quad + \left(k_r(s) + \psi''(s) - k_r^2(s)\psi(s)\right)\hat{n} + O\left(\psi^2(s)\right). \end{aligned}$$

Consider

$$\mathrm{d}s \to (1 - k_r(s)\psi(s))\mathrm{d}s + O\left(\psi^2(s)\right),$$

we have

$$\begin{aligned} k_r^2(s)\mathrm{d}s \to k_r^2(s)\mathrm{d}s &+ k_r^3(s)\psi(s)\mathrm{d}s + 2k_r(s)\psi''(s)\mathrm{d}s \\ &+ O\left(\psi^2(s)\right). \end{aligned}$$

The first order variation of $\oint k_r^2(s)\mathrm{d}s$ is therefore

$$\begin{aligned} \delta^{(1)}\oint k_r^2(s)\mathrm{d}s &= \oint \mathrm{d}s\, k_r^3(s)\psi(s) + \oint \mathrm{d}s\, 2k_r(s)\psi''(s), \\ &= \oint \mathrm{d}s\, k_r^3(s)\psi(s) + \oint \mathrm{d}s\, 2k''_r(s)\psi(s). \end{aligned} \tag{A4}$$

3. $\delta^{(1)}\int \mathrm{d}A$

As shown in Fig. 5, $\mathrm{d}A = \hat{e}_z \cdot |\vec{r} \times \mathrm{d}\vec{r}|/2 = \hat{e}_z \cdot |\vec{r}(s) \times \hat{t}(s)|\mathrm{d}s/2$, with the distorsion, the $\mathrm{d}A$ changes to

$$\begin{aligned} \mathrm{d}A \to \frac{\hat{e}_z}{2} \cdot \mathrm{d}s\big[&(1 - 2k_r(s)\psi(s))\vec{r}(s) \times \hat{t}(s) + \psi'(s)\vec{r}(s) \\ &\times \hat{n}(s) + \psi(s)\hat{e}_z\big] + O\left(\psi^2(s)\right). \end{aligned}$$

Thus,

$$\begin{aligned} \int \mathrm{d}A \to \frac{\hat{e}_z}{2} \cdot \oint \mathrm{d}s\big[&(1 - 2k_r(s)\psi(s))\vec{r}(s) \times \hat{t}(s) \\ &+ \psi'(s)\vec{r}(s) \times \hat{n}(s) + \psi(s)\hat{e}_z\big] + O\left(\psi^2(s)\right) \\ = \frac{\hat{e}_z}{2} \cdot \oint \mathrm{d}s\big[&(1 - 2k_r(s)\psi(s))\vec{r}(s) \times \hat{t}(s) - \psi(s)(\vec{r}(s) \\ &\times \hat{n}(s))' + \psi(s)\hat{e}_z\big] + O\left(\psi^2(s)\right), \\ = \int \mathrm{d}A + \oint &\psi(s)\mathrm{d}s + O\left(\psi^2(s)\right). \end{aligned} \tag{A5}$$

Therefore

$$\delta^{(1)}\int \mathrm{d}A = \oint \psi(s)\mathrm{d}s.$$

APPENDIX B: THE DERIVING OF $k_{r,n}(\theta)$

Equation (9)

$$\frac{\mathrm{d}k_r}{\sqrt{\alpha k_r - \beta k_r^3}} = \frac{\mathrm{d}\theta}{k_r}, \quad \alpha > 0, \quad k_r > 0,\ \beta = 1/4, \tag{B1}$$

can be rewritten as

$$\frac{k_r \mathrm{d}k_r}{\sqrt{\alpha}\sqrt{1 - k_r^3/(4\alpha)}} = \mathrm{d}\theta, \tag{B2}$$

which can be reduced to

$$\frac{\mathrm{d}\left(k_r^{3/2}\right)}{\sqrt{1 - \left(k_r^{3/2}\right)^2/(4\alpha)}} = \sqrt{\alpha}\mathrm{d}\theta. \tag{B3}$$

Integrating the terms on both sides, we have the approximate expression of $k_{r,n}(\theta)$ as

$$k_{r,n}(\theta) = (4\alpha)^{1/3}\sin^{2/3}[3(\theta + c_1(n))/4]. \tag{B4}$$

Since $k_{r,n} = 0$, at $\theta = \pi/2 + \pi/n$ for the critical shape, we have $c_1(n) = 5\pi/6 - \pi/n$. Then α can be determined based on Eq. (10). The explicit expression of $k_{r,n}(\theta)$ is shown in Eq. (11).

APPENDIX C: THE DERIVING OF EQ. (12)

The curvature $k_{r,n}(\theta)$ is the approximate explicit solution of Eqs. (7) and (8), which plays the center role in determining the parametric equations for the curve $\mathcal{C}$ for $n = 2$.

The curve $\mathcal{C}$ ($n = 2$) can be expressed as

$$\begin{aligned} x_2(s) &= x_2(0) + \int_0^s \mathrm{d}\tilde{s}\, x_2'(\tilde{s}) = x_2(0) + \int_0^s \mathrm{d}\tilde{s}\cos(\tilde{s}), \\ y_2(s) &= \int_0^s \mathrm{d}\tilde{s}\sin(\tilde{s}). \end{aligned} \tag{C1}$$

Here, s is the arc parameter. The origin is set at the center of the cross section, and $x_2(s = \pi/2) = 0$, $y_2(0) = 0$. According to the definition of the curvature of the curve, $k_r \equiv \mathrm{d}\theta/\mathrm{d}s$, the line element can be described by

$$d\tilde{s} = \frac{d\tilde{s}}{d\theta}d\theta = \frac{1}{k_r}d\theta,$$

the equation can be further reduced to

$$\begin{aligned} x_2(\theta) &= x_2(0) + \int_{\pi/2}^{\theta} d\tilde{\theta}\, \frac{\cos\tilde{\theta}}{k_{r,2}(\tilde{\theta})}, \\ y_2(\theta) &= \int_{\pi/2}^{\theta} d\tilde{\theta}\, \frac{\sin\tilde{\theta}}{k_{r,2}(\tilde{\theta})}. \end{aligned} \tag{C2}$$

Substitute the explicit expression of $k_{r,2}(\theta)$ to the above equation and integrate, we can obtain Eq. (12).

[1]R. Saito, M. S. Dresselhaus, and G. Dresselhaus, *Physical Properties of Carbon Nanotubes* (Imperial College Press, London, 1998).
[2]A. Jorio, M. S. Dresselhaus, and G. Dresselhaus, *Carbon Nanotubes* (Springer, Berlin, 2008).
[3]J. Tang, L.-C. Qin, T. Sasaki, M. Yudasaka, A. Matsushita, and S. Iijima, Phys. Rev. Lett. **85**, 1887 (2000).
[4]B. Anis, K. Haubner, F. Börrnert, L. Dunsch, M. H. Römmeli, and C. A. Kuntscher, Phys. Rev. B **86**, 155454 (2012).
[5]M. M. J. Treacy, T. W. Ebbesen, and J. M. Gibson, Nature (London) **381**, 678 (1996).
[6]M. Yao, Z. Wang, B. Liu, Y. Zou, S. Yu, W. Lin, Y. Hou, S. Pan, M. Jin, B. Zou, T. Cui, G. Zou, and B. Sundqvist, Phys. Rev. B **78**, 205411 (2008).
[7]C. Caillier, D. Machon, A. San-Miguel, R. Arenal, G. Montagnac, H. Cardon, M. Kalbac, M. Zukalova, and L. Kavan, Phys. Rev. B **77**, 125418 (2008).
[8]G. Gao, T. Cagin, and W. A. Goddard, Nanotechnology **9**, 184 (1998).
[9]A. L. Aguiar, E. B. Barros, R. B. Capaz, A. G. S. Filho, P. T. C. Freire, J. M. Filho, D. Machon, C. Caillier, Y. A. Kim, H. Muramatsu, M. Endo, and A. San-Miguel, J. Phys. Chem. C **115**, 5378 (2011).
[10]J. A. Elliott, J. K. W. Sandler, A. H. Windle, R. J. Young, and M. S. P. Shaffer, Phys. Rev. Lett. **92**, 095501 (2004).
[11]M. H. F. Sluiter and Y. Kawazoe, Phys. Rev. B **69**, 224111 (2004).
[12]P. Tangney, R. B. Capaz, C. D. Spataru, M. L. Cohen, and S. G. Louie, Nano. Lett. **5**, 2268 (2005).
[13]A. N. Imtani and V. K. Jindal, Phys. Rev. B **76**, 195447 (2007).
[14]W. Yang, R.-Z. Wang, Y.-F. Wang, X.-M. Song, B. Wang, and H. Yan, Phys. Rev. B **76**, 033402 (2007).
[15]J. Zang, A. Treibergs, Y. Han, and Z. F. Liu, Phys. Rev. Lett. **92**, 105501 (2004).
[16]D. Y. Sun, D. J. Shu, M. Ji, F. Liu, M. Wang, and X. G. Gong, Phys. Rev. B **70**, 165417 (2004).
[17]J. Z. Cai, L. Lu, W. J. Kong, H. W. Zhu, C. Zhang, B. Q. Wei, D. H. Wu, and F. Liu, Phys. Rev. Lett. **97**, 026402 (2006).
[18]J. Tang, L.-C. Qin, T. Sasaki, M. Yudasaka, A. Matsushita, and S. Iijima, J. Phys.: Condens. Matter **14**, 110575 (2002).
[19]K. Thirunavukkuarasu, F. Hennrich, K. Kamaras, and C. A. Kuntscher, Phys. Rev. B **81**, 045424 (2010).
[20]S. Park, D. Srivastava, and K. Cho, Nano Lett. **3**, 1273 (2003).
[21]K. Mylvaganam and L. C. Zhang, Nanotechnology **17**, 410 (2006).
[22]Y.-F. Zhang and Z.-F. Liu, Carbon **44**, 928 (2006).
[23]J. Kong, N. R. Franklin, C. Zhou, M. G. Chapline, S. Peng, K. Cho, and H. Dai, Science **287**, 622 (2000).
[24]B. I. Yakobson, C. J. Brabec, and J. Bernholc, J. Comput.-Aided Mater. Des. **3**, 173 (1996).
[25]B. I. Yakobson, C. J. Brabec, and J. Bernholc, Phys. Rev. Lett. **76**, 2511 (1996).
[26]T. C. Chang and Z. R. Guo, Nano Lett. **10**, 3490 (2010).
[27]O. E. Shklyaev, E. Mockensturm, and V. H. Crespi, Phys. Rev. Lett. **106**, 155501 (2011).
[28]J. Liu, Arch. Appl. Mech. **82**, 767 (2012).
[29]R. Martel, T. Schmidt, H. R. Shea, T. Hertel, and P. Avouris, Appl. Phys. Lett. **73**, 2447 (1998).
[30]P. E. Lammert, P. H. Zhang, and V. H. Crespi, Phys. Rev. Lett. **84**, 2453 (2000).
[31]J. Tersoff and R. S. Ruoff, Phys. Rev. Lett. **73**, 676 (1994).
[32]W. Mu, M. Li, W. Wang, and Z-c. Ou-Yang, New J. Phys. **11**, 113049 (2009).
[33]O.-Y. Zhong-can, Z. B. Su, and C. L. Wang, Phys. Rev. Lett. **78**, 4055 (1997).
[34]M. Abramowitz and I. Stegun, *Handbook of Mathematical Functions*, Ninth Printing (Dover Publications, Inc., New York, 1972).
[35]W. Mu, G. Zhang, and Z.-C. Ou-Yang, Jpn. J. Appl. Phys., Part 1 **51**, 065101 (2012).
[36]W. Mu and Z.-C. Ou-Yang, "Chirality dependent elasticity of single walled carbon nanotubes," in *Nanowires: Properties, Synthesis, and Applications*, edited by V. Lefevre (Nova Science Publishers, Inc., Hauppauge, 2012), pp. 160–170.
[37]W. Mu, G. Zhang, and Z.-C. Ou-Yang, Appl. Phys. Lett. **103**, 053112 (2013).
[38]J. Wu and J. Cao, J. Phys. Chem. B **109**, 21342 (2005).
[39]J. Wu and J. Cao, Physica A **371**, 249 (2006).
[40]Z.-C. Ou-Yang, J.-X. Liu, and Y.-Z. Xie, *Geometric Methods in the Elastic Theory of Membranes in Liquid Crystal Phases*, 1st ed., Advanced Series on Theoretical Physical Science Vol. 2 (World Scientific Publishing Company, Singapore, 1999).
[41]X.-H. Zhou, Int. J. Mod. Phys. B **24**, 587 (2010).